

# Stability of Metal–Carbon Bond versus Metal Reduction during Ethylene Polymerization Promoted by a Vanadium Complex: The Role of the Aluminum Cocatalyst

Khalil Feghali, David J. Harding, Damien Reardon, Sandro Gambarotta,\* and Glenn Yap

Department of Chemistry, University of Ottawa, Ottawa, Ontario K1N 6N5, Canada

Qinyan Wang

NOVA Chemicals, 2928 16th Street, N.E. Calgary, Alberta T2E 7K7, Canada

Received December 6, 2001

The dinuclear and trivalent complex  $\{[(\text{Me}_3\text{Si})\text{NCH}_2\text{CH}_2]_2\text{N}(\text{Me}_3\text{Si})\}_2\text{V}_2(\mu\text{-Cl})_2$  (**1**) is the precursor to mono- and dinuclear alkyl derivatives that are thermally stable. For example, treatment with MeLi gives a stable methyl derivative, probably isostructural with **1**, which upon further treatment with pyridine affords the mononuclear complex  $\{[(\text{Me}_3\text{Si})\text{NCH}_2\text{CH}_2]_2\text{N}(\text{Me}_3\text{Si})\}\text{V}(\text{CH}_3)(\text{pyridine})$  (**2**). However, reaction of **1** with  $\text{Me}_2\text{AlCl}$ ,  $\text{AlMe}_3$ , or PMAO-IP yields the tetrametallic species  $\{[(\text{Me}_3\text{Si})\text{NCH}_2\text{CH}_2]_2\text{N}(\text{Me}_3\text{Si})\}_2\text{V}_2(\mu\text{-Cl})_2(\text{AlMe}_2)_2$  (**3**), where the central core of **1** was preserved except for the vanadium centers, which were reduced to the divalent state. The two  $\text{Me}_2\text{Al}$  residues remained coordinated to the amido ligand. The reduction of vanadium to the divalent state relates to the relatively short life of **1** as an ethylene polymerization catalyst. A similar reaction of **1** with  $\text{AlCl}_3$  resulted in disproportionation forming the tetravalent complex  $\{[(\text{Me}_3\text{Si})\text{NCH}_2\text{CH}_2]_2\text{N}(\text{Me}_3\text{Si})\}\text{VCl}_2\text{AlCl}_3$  (**4**) and the pentanuclear mixed-valent V(II)/V(III) species  $[(\text{AlCl}_2)\{[(\text{Me}_3\text{Si})\text{NCH}_2\text{CH}_2]_2\text{N}(\text{Me}_3\text{Si})\}\text{V}]_2\text{-}[(\mu\text{-Cl})_6\text{V}]\cdot(\text{toluene})_2$  (**5**). The fact that complex **5** contains a divalent vanadium atom stripped of its ligand system indicates that two different reaction mechanisms are operating to reduce the vanadium center and that the differing Lewis acidity of the two aluminum species is the determining factor.

## Introduction

Research into the area of Ziegler–Natta olefin polymerization has traditionally focused on the group 4 metals since these catalysts tend to be both efficient and selective.<sup>1</sup> In addition, most of the industrially successful catalysts are based on Cp and its derivatives, as these ligands are both robust and highly tunable. Nevertheless, some nonmetallocene systems have found industrial applications. Particularly relevant to this work is the V(*acac*)<sub>3</sub> catalyst used for the commercial production of ethylene-propylene-diene elastomers (EPDM).<sup>2</sup>

A recent study of this system in our group highlighted a number of problems with the process.<sup>3</sup> The investigation confirmed that the Al cocatalyst plays a pivotal role

in the catalyst activation by generating, in addition to the V–R function, empty coordination sites on vana-

(2) See for example: (a) Doi, Y.; Suzuki, S.; Soga, K. *Macromolecules* **1986**, *19*, 2896. (b) Ooumi, T.; Soga, K. *Makromol. Chem.* **1992**, *193*, 823. (c) Gumbolt, A.; Helberg, J.; Schleitzer, G. *Makromol. Chem.* **1967**, *101*, 229. (d) Adisson, E. *J. Polym. Sci., Part A: Polym. Chem.* **1994**, *32*, 1033. (e) Davis, S. C.; von Hellens, W.; Zahalka, H. In *Polymer Material Encyclopedia Vol. 3*; Salamone, J. C., Ed.; CRC Press Inc.: Boca Raton, FL, 1996. (f) Sinn, H.; Kaminski, W. In *Advances in Organometallic Chemistry*; Stone, F. G. A., West, R., Eds.; Academic Press: New York, 1980. (g) Doi, Y.; Tokuhiko, N.; Nunomura, M.; Miyake, H.; Suuki, S.; Soga, K. *Transition Metals and Organometallics as Catalysts for Olefin Polymerization*; Kaminsky, W., Sinn H., Eds.; Springer-Verlag: Berlin, 1988. (h) Carrick, W. L. *J. Am. Chem. Soc.* **1958**, *80*, 6455. (i) Christman, D. L. *J. Polym. Sci.* **1972**, *A-1*, 471. (j) Pasquon, I. G.; Giannini, U. In *Catalysis*; Anderson, J. R., Boudart, M., Eds.; Springer-Verlag: Berlin, 1984. (k) Carrick, W. L.; Kluiber, R. W.; Bonner, E. F.; Wartman, L. H.; Rugg, F. M.; Smith J. J. *J. Am. Chem. Soc.* **1960**, *82*, 3883. (l) Lehr, M. H. *Macromolecules* **1968**, *1*, 178. (m) Christman, D. L.; Keim, G. I. *Macromolecules* **1968**, *1*, 358. (n) Lehr, M. H.; Carmen, C. J. *Macromolecules* **1969**, *2*, 217. (o) Duck, E. W.; Grant, D.; Horder, J. R.; Jenkins, D. K.; Marlow, A. E.; Wallis, S. R.; Doughty, A. G.; Maradon, J. M.; Skinner, G. A. *Eur. Polym. J.* **1974**, *10*, 481. (p) Schuere, S.; Fisher, J.; Kress, J. *Organometallics* **1995**, *14*, 2627. (q) Feher, F. J.; Blanski, R. L. *J. Am. Chem. Soc.* **1992**, *114*, 5886. (r) Feher, F. J.; Walzer, J. F.; Blanski, R. L. *J. Am. Chem. Soc.* **1991**, *113*, 3618. (s) Feher, F. J.; Blanski, R. L. *Organometallics* **1993**, *12*, 958. (t) Cucinella, S.; Mazzei A. U.S. Patent 3,711,455, Cl. 260–85.3, 1973. (u) Boor, J., Jr.; Youngman, E. A. *J. Polym. Sci. A* **1966**, *4*, 1861. (v) Zambelli, A.; Proto, A.; Longo, P. In *Ziegler Natta Catalysis*; Fink, G., Mulhaupt, R., Brintzinger, H. H., Eds.; Springer-Verlag: Berlin, 1995.

(3) Ma, Y.; Reardon, D. F.; Gambarotta, S.; Yap, G. P. A. *Organometallics* **1999**, *18*, 2773.

(1) See for example: (a) Mohring, P. C.; Coville, N. J. *J. Organomet. Chem.* **1994**, *479*, 1. (b) Erker, G.; Nolte, R.; Tsay, Y. H.; Kruger, C. *Angew. Chem.* **1989**, *28*, 628. (c) Erker, G.; Nolte, R.; Aul, R.; Wilker, S.; Kruger, C.; Noe, R. *J. Am. Chem. Soc.* **1991**, *113*, 7594. (d) Kaminsky, W.; Kulper, K.; Brintzinger, H. H.; Wild, R. W. P. *Angew. Chem., Int. Ed. Engl.* **1985**, *6*, 507. (e) Coates, G. W.; Weymouth, R. M. *J. Am. Chem. Soc.* **1991**, *113*, 6270. (f) Ewen, J. A. *J. Am. Chem. Soc.* **1984**, *106*, 6355. (g) Guerra, G.; Cavallo, L.; Moscardi, G.; Vacatello, M.; Corradini, P. *J. Am. Chem. Soc.* **1994**, *116*, 2988. (h) Jordan, R. F. *Adv. Organomet. Chem.* **1991**, *32*, 325. (i) Brintzinger, H. H.; Fisher, D.; Mulhaupt, R.; Rieger, B.; Waymouth, R. M. *Angew. Chem., Int. Ed. Engl.* **1995**, *34*, 1143. (j) Bochmann, M. *J. Chem. Soc., Dalton Trans.* **1996**, 255.

dium (otherwise coordinatively saturated) via removal of one or more of the *acac* ligands. However, by stripping the metal of the remaining *acac* ligands, the cocatalyst decreases the stability of the V–R bond. Consequently, the vanadium metal is rapidly reduced to the divalent state, resulting in complete catalyst deactivation. Despite this drawback, vanadium catalysts remain irreplaceable in EPDM manufacture. Thus, we were interested in developing new catalysts that might avoid the problems encountered with the above system. To prevent ligand leaching, it was decided to change the donor set from oxygen to nitrogen atoms. With such a system one might reasonably expect that the lower affinity of aluminum for nitrogen would reduce migration of the ligand from the vanadium center.

A direct consequence of ligand leaching is the reduction of the metal to V(II), which is a rather common deactivation pathway for vanadium catalysts. This is thought to be a result of a variety of events including  $\beta$ -H elimination of the alkyl polymer growing chain<sup>4</sup> and C–H  $\sigma$ -bond metathesis<sup>4</sup> and relates to an intrinsic instability of the V–C bond once the ligand system has been abstracted from the vanadium center. Although a number of V(III) alkyl complexes have been successfully synthesized,<sup>5,6</sup> nevertheless, these complexes generally employ sterically bulky alkyl ligands or bulky supporting ligands. By analogy, we felt that a large chelating ligand would also be desirable for a vanadium catalyst since it should extend the catalyst's life. Moreover, it was hoped that a polydentate chelating ligand might also contribute to the aggregation of both vanadium and aluminum in the same molecular structure, providing insight into the catalyst/cocatalyst interaction.

In view of these considerations the bulky *N,N,N*-tris(trimethylsilyl)diethylenediamidoamino ligand<sup>7</sup> was selected for this study, as it has already been successfully employed for different purposes, including one spectacular case of dinitrogen cleavage,<sup>8</sup> with a range of metals including V,<sup>6</sup> Ti,<sup>9</sup> Zr,<sup>10</sup> and Nb.<sup>11</sup> The resulting vanadium complexes prepared in the course of this investigation and their catalytic behavior, including their interaction with the Al cocatalyst, are now presented.

(4) Guram, A. S.; Jordan, R. F. In *Comprehensive Organometallic Chemistry*; Abel, E. W., Stone, F. G. A., Wilkinson, G., Eds. Pergamon: New York, 1995, and references therein.

(5) Non-Cp and stable vanadium alkyls are rare compounds: (a) Seidel, W., Kreiseli, G. *Z. Anorg. Allg. Chem.*, **1977**, *435*, 146. (b) Gambarotta, S.; Floriani, C.; Chiesi-Villa, A.; Guastini, G. *J. Chem. Soc., Dalton Trans.* **1984**, 886. (c) Gambarotta, S.; Mazzanti, M.; Floriani, C.; Chiesi-Villa, A.; Guastini, G. *J. Chem. Soc., Dalton Trans.* **1985**, 829. (d) Solari, E.; De Angelis, S.; Floriani, C.; Chiesi-Villa, A.; Rizzoli, C. *Inorg. Chem.* **1992**, *31*, 96. (e) Wills, A. R.; Edwards, P. G. *J. Chem. Soc., Dalton Trans.* **1989**, 1253. (f) Gambarotta, S.; Floriani, C.; Chiesi-Villa, A.; Guastini, G. *J. Chem. Soc., Chem. Commun.* **1984**, 886. (g) Buijink, J. K.; Meetsma, A.; Teuben, J. H. *Organometallics* **1993**, *12*, 2004. (h) Berno, P.; Gambarotta, S.; Richeson, D. In *Comprehensive Organometallic Chemistry II*; Abel, E. W., Stone, F. G. A., Wilkinson, G., Eds.; Oxford 1995, and references therein.

(6) Clancey, G. P.; Clark, H. C. S.; Clentsmith, G. K. B.; Hitchcock, P. B.; Cloke, F. G. N. *J. Chem. Soc., Dalton Trans.* **1999**, 3345.

(7) Gol'din, G. S.; Baturina, L. S.; Gavrilova, T. *Zh. Obshch. Khim.* **1975**, *45*, 2189.

(8) Clentsmith, G. K. B.; Bates, V. M. E.; Hitchcock, P. B.; Cloke, F. G. N. *J. Am. Chem. Soc.* **1999**, *121*, 10444.

(9) (a) Cloke, F. G. N.; Love, J. B.; Hitchcock, P. B. *J. Chem. Soc., Dalton Trans.* **1995**, 25. (b) Love, J. B.; Clark, H. C. S.; Cloke, F. G. N.; Green, J. C.; Hitchcock, P. B. *J. Am. Chem. Soc.* **1999**, *121*, 6843.

(10) Clark, H. C. S.; Cloke, F. G. N.; Hitchcock, P. B.; Love, J. B.; Wainright, A. P. *J. Organomet. Chem.* **1995**, *503*, 333.

(11) Horton, A. D.; De With, J.; Van de Linden, A. J.; Van de Weg, H. *Organometallics* **1996**, *15*, 2672.

## Experimental Section

All operations were performed under inert atmosphere by using standard Schlenk type techniques. Polymethylalumoxane solution (13.5% Al) in toluene (PMAO-IP, Akzo-Nobel), AlMe<sub>3</sub> (Aldrich), and Me<sub>2</sub>AlCl (Aldrich) were used as received without further purification. VCl<sub>3</sub>(THF)<sub>3</sub><sup>12</sup> and [(Me<sub>3</sub>Si)NHCH<sub>2</sub>CH<sub>2</sub>]<sub>2</sub>N(Me<sub>3</sub>Si)<sup>7</sup> were synthesized according to published procedures. The corresponding dilithium salt and complex **1** were prepared by a slight modification of the procedure described by Cloke.<sup>6,8–10</sup> AlCl<sub>3</sub> was sublimed under reduced pressure before use. Infrared spectra were recorded on a Mattson 9000 and Nicolet 750-Magna FTIR instruments from Nujol mulls prepared in a drybox. Samples for magnetic susceptibility measurements were weighed inside a drybox equipped with an analytical balance and sealed into calibrated tubes. Magnetic measurements were carried out with a Gouy balance (Johnson Matthey) at room temperature. Magnetic moments were calculated following standard methods,<sup>13</sup> and corrections for underlying diamagnetism were applied to the data.<sup>14</sup> Elemental analyses were carried out using a Perkin-Elmer 2400 CHN analyzer. NMR analysis were carried out on Varian Gemini 200 and Bruker AMX-500 spectrometers using vacuum-sealed NMR tubes prepared inside a drybox.

**Preparation of [(Me<sub>3</sub>Si)NLi<sub>2</sub>CH<sub>2</sub>CH<sub>2</sub>]<sub>2</sub>N(Me<sub>3</sub>Si).** The addition of butyllithium (52 mL, 0.13 mol, 2.5 M) to a solution of [(Me<sub>3</sub>Si)NHCH<sub>2</sub>CH<sub>2</sub>]<sub>2</sub>N(Me<sub>3</sub>Si) (21 g, 0.065 mol) in hexane (150 mL) at –80 °C afforded a white precipitate. The solution was allowed to warm to room temperature, stirred for 1 h, and filtered to collect the dilithiated salt (19.3 g, 0.058 mol, 89%). IR (Nujol mull, KBr, cm<sup>-1</sup>):  $\nu$  1258 (m), 1083 (m), 944 (w), 884 (w), 825 (m), 729 (w). <sup>1</sup>H NMR (CDCl<sub>3</sub>, 200 MHz, 25 °C):  $\delta$  0.15 (s, 9H, TMS), 0.34 (s, 18H, TMS), 2.9 (m, 4H, CH<sub>ethyl</sub>).

**Preparation of {[(Me<sub>3</sub>Si)NCH<sub>2</sub>CH<sub>2</sub>]<sub>2</sub>N(Me<sub>3</sub>Si)}<sub>2</sub>V<sub>2</sub>( $\mu$ -Cl)<sub>2</sub> (**1**).** A solution of VCl<sub>3</sub>(THF)<sub>3</sub> (5.8 g, 15.5 mmol) in THF (100 mL) was treated with 1 equiv of [(Me<sub>3</sub>Si)NLi<sub>2</sub>CH<sub>2</sub>CH<sub>2</sub>]<sub>2</sub>N(Me<sub>3</sub>Si) (5.2 g, 15.5 mmol) at room temperature. The red-orange color of the solution immediately darkened upon mixing, and stirring was continued for 30 min. THF was removed in vacuo, and the resulting red powder was redissolved in hexane (150 mL). The solution was then filtered to eliminate LiCl and allowed to stand at 0 °C, for 24 h, upon which dark red crystals of **1** separated (5.1 g, 6.2 mmol, 80%). IR (Nujol mull, KBr, cm<sup>-1</sup>):  $\nu$  1377 (m), 1250 (s), 1074 (s), 937 (s), 911 (s), 825 (s).  $\mu_{\text{eff}}$ : 2.93  $\mu_{\text{B}}$ . Anal. Calcd for C<sub>26</sub>H<sub>70</sub>N<sub>6</sub>Si<sub>6</sub>V<sub>2</sub>Cl<sub>2</sub> (found): C, 38.64 (38.53); H, 8.73 (8.61); N, 10.40 (10.34).

**Preparation of {[(Me<sub>3</sub>Si)NCH<sub>2</sub>CH<sub>2</sub>]<sub>2</sub>N(Me<sub>3</sub>Si)}V(CH<sub>3</sub>)-pyridine (**2**).** A solution of {[(Me<sub>3</sub>Si)NCH<sub>2</sub>CH<sub>2</sub>]<sub>2</sub>N(Me<sub>3</sub>Si)}<sub>2</sub>V<sub>2</sub>( $\mu$ -Cl)<sub>2</sub> (1.1 g, 1.4 mmol) in ether (100 mL) was treated with 1 equiv of methyllithium (2 mL, 1.4 M) at room temperature. After mixing, the color of the solution changed to pink-red and stirring was continued for 30 min. The solvent was removed in vacuo, the solid residue was redissolved in hexane (50 mL), and the solution was filtered to eliminate LiCl. A small portion of the red solid was used for a Toepler pump degradation experiment (0.5 g of dry solid was dissolved in toluene (15 mL) and treated with 3 equiv of gaseous HCl; methane gas was collected with a Topler pump recovering 57 mL at 40 mmHg and 298 K). The addition of dry pyridine (5 mL) turned the color of the solution purple. The mixture was allowed to stand at –80 °C for 36 h, upon which large dark purple crystals of **2** separated (0.98 g, 2.1 mmol, 75%).  $\mu_{\text{eff}}$ : 2.90  $\mu_{\text{B}}$ . The extreme air-sensitivity prevented combustion analysis determinations.

**Preparation of {[(Me<sub>3</sub>Si)NCH<sub>2</sub>CH<sub>2</sub>]<sub>2</sub>N(Me<sub>3</sub>Si)}<sub>2</sub>V<sub>2</sub>( $\mu$ -Cl)<sub>2</sub>(AlMe<sub>2</sub>)<sub>2</sub> (**3**), Method A.** A solution of **1** (0.9 g, 1.14 mmol)

(12) Manzer, L. E. *Inorg. Synth.* **1982**, *21*, 138.

(13) Mabbs, M. B.; Machin, D. *Magnetism and Transition Metal Complexes*; Chapman and Hall: London, 1973.

(14) Foese, G.; Gorter, C. J.; Smits, L. J. *Constantes Selectionnées Diamagnetisme, Paramagnetisme, Relaxation Paramagnetique*; Masson: Paris, 1957.



in hexane (100 mL) was treated with 1 mL of PMAO (13% Al solution in toluene) at room temperature. Upon addition, a green precipitate separated from the red solution. It took roughly 54 equiv of Al (PMAO) to yield a colorless solution. Crystals of **3** were grown by layering a solution of PMAO in toluene over a solution of **1** in hexane and subsequent standing at room temperature for 3 days (0.2 g, 0.22 mmol, 19%). IR (Nujol, KBr,  $\text{cm}^{-1}$ ):  $\nu$  2722 (w), 2701 (w), 1377 (m), 1247 (s), 1197 (s), 1126 (m), 1099 (s), 1054 (s), 904 (s), 836 (s), 765 (s), 674 (s).  $\mu_{\text{eff}}$ : 3.9  $\mu_{\text{B}}$ . Anal. Calcd for  $\text{C}_{30}\text{H}_{82}\text{N}_6\text{Si}_6\text{V}_2\text{Al}_2\text{Cl}_2$  (found): C 39.07(38.88); H 8.96 (8.71); N 9.11 (8.97).

**Method B.** A solution of **1** (1.2 g, 1.6 mmol) in hexane (150 mL) was treated with 2 equiv of a solution of  $\text{Me}_3\text{Al}$  in hexane (3 mL, 2.0 M) and at room temperature. After mixing the color of the solution changed to dark red and stirring was continued for 30 min. The mixture was allowed to stand at 4 °C, for 2 days, upon which emerald-green crystals of **3** separated from a brown solution (0.9 g, 0.99 mmol, 60%).

**Method C.** Same procedure and amount as method A but using  $\text{Me}_2\text{AlCl}$  (yield 21%).

**Isolation of  $\{[(\text{Me}_3\text{Si})\text{NCH}_2\text{CH}_2]_2\text{N}(\text{Me}_3\text{Si})\}_2\text{VCl}_2\text{AlCl}_3$  (**4**) and  $[(\text{AlCl}_2)\{[(\text{Me}_3\text{Si})\text{NCH}_2\text{CH}_2]_2\text{N}(\text{Me}_3\text{Si})\}_2\text{V}\}_2(\mu\text{-Cl})_6\text{V}] \cdot (\text{toluene})_2$  (**5**).** A solution of **1** (1.0 g, 1.23 mmol) in toluene (150 mL) was treated with 2 equiv of  $\text{AlCl}_3$  (0.37 g, 2.8 mmol) at room temperature. After mixing the color of the solution changed to brown and stirring was continued for 1 h. The solution was then filtered (to eliminate excess  $\text{AlCl}_3$ ), and the volume was reduced. The mixture was allowed to stand at room temperature, for 24 h, upon which red crystals of **4** separated (0.2 g, 0.35 mmol, 28%). IR (Nujol, KBr,  $\text{cm}^{-1}$ ):  $\nu$  1377 (m), 1255 (s), 1089 (m), 1051 (m), 1001 (m), 912 (s), 891 (s), 840 (s), 759 (m), 721 (w), 669 (w), 634 (w).  $\mu_{\text{eff}}$ : 1.83  $\mu_{\text{B}}$ . Anal. Calcd for  $\text{C}_{13}\text{H}_{35}\text{N}_3\text{Si}_3\text{VCl}_5\text{Al}$  (found): C 27.26 (27.17); H 6.16 (6.12); N 7.33 (7.28). Further concentration of the mother liquors afforded another crop of crystalline **4**. Among the red crystals thin green plates were present. X-ray analysis of the latter confirmed the molecular connectivity of **5**. Unfortunately, only small amounts of the complex were obtained and no further characterization was possible.

**Preparation of  $\{[(\text{Me}_3\text{Si})\text{NCH}_2\text{CH}_2]_2\text{N}(\text{Me}_3\text{Si})\}_2\text{VCl}_2$  (**6**).**  
**Method A.** A solution of **1** (1.0 g, 1.2 mmol) in toluene (150 mL) at room temperature was treated with 1 equiv of triphenylphosphonium dichloride (0.2 g, 0.6 mmol) per vanadium dimer. After mixing the color of the solution changed to brown and stirring was continued for 1 h. The solution was then filtered and the solvent was reduced to dryness. Freshly distilled hexane was added (30 mL). The mixture was allowed to stand at -40 °C, for 24 h, upon which brown crystals of **6** separated (0.2 g, 0.5 mmol, 41%). IR (Nujol, KBr,  $\text{cm}^{-1}$ ):  $\nu$  1377 (m), 1255 (s), 1089 (m), 1051 (m), 1001 (m), 912 (s), 891 (s), 840 (s), 759 (m), 721 (w), 669 (w), 634 (w).  $\mu_{\text{eff}}$ : 1.83  $\mu_{\text{B}}$ . Anal. Calcd for  $\text{C}_{13}\text{H}_{35}\text{N}_3\text{Si}_3\text{VCl}_2$  (found): C 35.52 (35.49); H 8.03 (7.95); N 9.58 (9.53).

**Method B.** A solution of  $[(\text{Me}_3\text{Si})\text{NLi}_2\text{CH}_2\text{CH}_2]_2\text{N}(\text{Me}_3\text{Si})$  (7.1 mmol) in ether (100 mL) was combined via cannula with a suspension of  $\text{VCl}_4(\text{DME})$  (2 g, 7.1 mmol) in ether (100 mL) over a period of 30 min. The resulting dark brown solution was allowed to stir overnight and was then filtered to eliminate LiCl. The volume of the solution was reduced and allowed to stand at -20 °C overnight, upon which crystals of **6** separated (2.1 g, 4.9 mmol, 69%).

**Reaction of Complex **1** with  $\text{VCl}_3(\text{THF})_3$ .** A dark red solution of **1** (0.57 g, 0.7 mmol) in toluene (30 mL) was mixed with a suspension of  $\text{VCl}_3(\text{THF})_3$  (0.54 g, 1.4 mmol) in the same solvent (70 mL). The mixture was stirred for 2 h, upon which the color changed to dark brown. The solvent was evaporated to dryness and replaced by 50 mL of freshly distilled diethyl ether. The solution was filtered and allowed to stand at -40 °C for 2 days, affording brown flat crystals of **6** (0.32 g; yield 51%). The ether-insoluble residue was redissolved in toluene and treated with 0.44 mL of TMEDA (0.34 g; 2.9 mmol), which

rapidly changed the color to dark blue. The solid was then identified as  $\text{VCl}_2(\text{TMEDA})_2$  (0.24 g, 38%) by comparison of the analytical and spectroscopic data with those of an analytically pure sample.

**Ethylene Polymerization.** A bench scale reactor was used in the polymerization experiments. The reactor uses a programmable logic control (PLC) system with Wonderware 5.1 software for process control. Ethylene polymerizations were performed in the 500 mL Autoclave Engineers Zipperclave reactor equipped with an air-driven stirrer and an automatic temperature control system. All the chemicals were fed into the reaction batchwise except for ethylene, which was fed on demand.

Conditions for polymerization:

	slurry phase	solution phase
toluene	216 mL	216 mL
catalyst concentration	300 $\mu\text{mol/L}$	300 $\mu\text{mol/L}$
$\text{Me}_2\text{AlCl}$	$\text{Al/V} = 60$ (mol/mol)	$\text{Al/V} = 60$ (mol/mol)
reaction temperature	50 °C	140 °C
reactor pressure	300 psig total	286 psig total

As summarized above the control temperature was 50 °C for a slurry polymerization and 140 °C for solution polymerization experiments. The polymerization time varied from 10 to 30 min. The reaction was terminated by adding 5 mL of methanol to the reactor, and the polymer was recovered by evaporation of the toluene in vacuo. The polymerization activities were calculated on the basis of weight of polymer produced.

Polymer molecular weights and molecular weight distributions were measured by GPC (Waters 150-C) at 140 °C in 1,2,4-trichlorobenzene calibrated using polystyrene standards. DSC was conducted on a DSC 220 C from Seiko Instruments. The heating rate was 10 °C/min from 0 to 200 °C.

In a typical polymerization experiment, the solvent was presaturated with ethylene in the reactor at the desired temperature. The cocatalyst was injected in the reactor followed by introduction of the precatalyst. Reproducibility of catalyst activity and reactor operation was checked by regularly running polymerization experiments using a standard zirconium catalyst and by repeating the experiments under identical reaction conditions. Errors and deviation were always below 5.9%.

**X-ray Crystallography. Structural Determination of **1**, **2**, **3**, **4**, and **5**.** Suitable crystals were selected, mounted on thin glass fibers using viscous oil, and cooled to the data collection temperature. Data were collected on a Bruker AX SMART 1k CCD diffractometer using 0.3°  $\omega$ -scans at 0°, 90°, and 180° in  $\phi$ . Unit-cell parameters were determined from 60 data frames collected at different sections of the Ewald sphere. Semiempirical absorption corrections based on equivalent reflections were applied.<sup>15</sup>

No symmetry higher than triclinic was evident from the diffraction data of **3** and **5**. Solution in the centric option yielded chemically reasonable and computationally stable results of refinement. Systematic absences in the diffraction data and unit-cell parameters were uniquely consistent for the reported space groups for **1**, **2**, and **4**. The structures were solved by direct methods, completed with difference Fourier syntheses, and refined with full-matrix least-squares procedures based on  $F^2$ . The compound molecules for **3** and **5** are located on inversion centers. Two toluene solvent molecules were located cocrystallized in the asymmetric unit of **5**. All non-hydrogen atoms were refined with anisotropic displacement parameters. All hydrogen atoms were treated as idealized contributions. All scattering factors are contained in the SHEXTL 5.10 program library (Sheldrick, G. M. Bruker AXS,

**Table 1. Crystal Data and Structure Analysis Results for Complexes 1, 2, and 3**

	1	2	3
formula	C <sub>26</sub> H <sub>70</sub> N <sub>6</sub> Cl <sub>2</sub> Si <sub>6</sub> V <sub>2</sub>	C <sub>19</sub> H <sub>43</sub> N <sub>4</sub> Si <sub>3</sub> V	C <sub>30</sub> H <sub>82</sub> Al <sub>2</sub> C <sub>12</sub> N <sub>6</sub> Si <sub>6</sub> V <sub>2</sub>
fw	808.20	462.78	922.30
space group	monoclinic, <i>P2(1)/c</i>	monoclinic, <i>P2(1)/n</i>	triclinic, <i>P1̄</i>
<i>a</i> (Å)	10.534(1)	10.7952(5)	10.433(2)
<i>b</i> (Å)	37.931(4)	16.6050(8)	11.260(2)
<i>c</i> (Å)	11.707(1)	14.7725(8)	12.639(3)
$\alpha$ (deg)	90	90	97.09(2)
$\beta$ (deg)	109.701(1)	93.228(1)	105.52(1)
$\gamma$ (deg)	90	90	115.10(1)
<i>V</i> (Å <sup>3</sup> )	4403.5(8)	2643.8(2)	1246.8(4)
<i>Z</i>	4	4	1
radiation (K $\alpha$ , Å)	0.71073	0.71073	0.71073
<i>T</i> (K)	223(2)	203(2)	203(2)
<i>D</i> <sub>calcd</sub> (g cm <sup>-3</sup> )	1.219	1.163	1.228
$\mu$ <sub>calcd</sub> (cm <sup>-1</sup> )	7.34	5.23	6.89
<i>F</i> <sub>000</sub>	1728	1000	494
<i>R</i> , <i>R</i> <sub>w</sub> <sup>2</sup> , <i>a</i> GoF	0.0725, 0.1597, 1.167	0.0609, 0.1250, 1.052	0.0639, 0.1962, 1.071

$$^a R = \sum F_o - F_c / \sum F_o R_w = [(\sum (F_o - F_c)^2 / \sum w F_o^2)]^{1/2}.$$

**Table 2. Crystal Data and Structure Analysis Results for Complexes 4 and 5**

	4	5
formula	C <sub>13</sub> H <sub>35</sub> AlCl <sub>5</sub> N <sub>3</sub> Si <sub>3</sub> V	C <sub>40</sub> H <sub>86</sub> Al <sub>2</sub> Cl <sub>10</sub> N <sub>6</sub> Si <sub>6</sub> V <sub>3</sub>
fw	572.88	1380.97
space group	monoclinic, <i>P2(1)/c</i>	triclinic, <i>P1̄</i>
<i>a</i> (Å)	9.373(5)	10.476(5)
<i>b</i> (Å)	20.215(9)	11.647(7)
<i>c</i> (Å)	14.794(7)	15.177(6)
$\alpha$ (deg)	90	69.75(3)
$\beta$ (deg)	97.950(5)	87.53(5)
$\gamma$ (deg)	90	73.54(5)
<i>V</i> (Å <sup>3</sup> )	2776(2)	1663(1)
<i>Z</i>	4	1
radiation (K $\alpha$ , Å)	0.71073	0.71073
<i>T</i> (K)	203(2)	203(2)
<i>D</i> <sub>calcd</sub> (g cm <sup>-3</sup> )	1.371	1.379
$\mu$ <sub>calcd</sub> (cm <sup>-1</sup> )	10.06	9.82
<i>F</i> <sub>000</sub>	1188	717
<i>R</i> , <i>R</i> <sub>w</sub> <sup>2</sup> , <i>a</i> GoF	0.0509, 0.1094, 1.065	0.0638, 0.1049, 1.055

$$^a R = \sum F_o - F_c / \sum F_o R_w = [(\sum (F_o - F_c)^2 / \sum w F_o^2)]^{1/2}.$$

Madison, WI, 1997). Crystallographic data and relevant bond distances and angles are given in Tables 1–4.

**Complex 1.** The crystal structure of **1** (Figure 1) shows a symmetry-generated bimetallic complex with two distorted trigonal bipyramidal vanadium(III) centers bridged by two chlorides [V(1)–Cl(1)–V(2) = 97.36(6)°, V(1)–Cl(2)–V(2) = 97.44(6)°, Cl(2)–V(1)–Cl(1) = 82.03(6)°, Cl(2)–V(2)–Cl(1) = 82.11(6)°]. The equatorial plane of the trigonal bipyramidal vanadium is defined by the ligand's two terminal nitrogens and a bridging chlorine atom [N(1)–V(1)–N(3) = 117.91(26)°, N(1)–V(1)–N(2) = 84.69(22)°, N(1)–V(1)–Cl(1) = 119.98(19)°, N(1)–V(1)–Cl(2) = 100.98(17)°, N(4)–V(2)–N(6) = 118.03–(24)°, N(4)–V(2)–N(5) = 84.76(21)°, N(4)–V(2)–Cl(1) = 100.72–(17)°, N(4)–V(2)–Cl(2) = 121.96(18)°]. The central ligand nitrogen atom and the second bridging chlorine atom [N(2)–V(1)–Cl(2) = 174.21(16)°, N(5)–V(2)–Cl(1) = 173.79(15)°] occupy the axial positions. The V–Cl distances are effectively equivalent and fall into the expected range for bridging chlorides [V(1)–Cl(1) = 2.373(2) Å, V(1)–Cl(2) = 2.459(2) Å, V(2)–Cl(1) = 2.462(2) Å, V(2)–Cl(2) = 2.373(2) Å]. The V–N bond lengths are as expected for the silylamido donors [V(1)–N(1) = 1.906(5) Å, V(1)–N(3) = 1.899(5) Å, V(2)–N(4) = 1.905–(5) Å, V(1)–N(6) = 1.902(5) Å], while the longer V–N bond length formed by the central nitrogen is indicative of a coordinatively bound nitrogen [V(1)–N(2) = 2.179(5) Å, V(2)–N(5) = 2.193(5) Å]. All other bond distances and angles are as expected.

**Complex 2.** The complex is monomeric and features a trigonal bipyramidal vanadium atom (Figure 2). The coordina-

tion geometry is defined by a methyl group [V–C = 2.118(3) Å] and the nitrogen atom of one coordinated molecule of pyridine [V–N = 2.157(2) Å], while the other three coordination sites are occupied by the ligand nitrogen atoms. The equatorial plane is occupied by the two terminal nitrogen atoms of the amido ligand and by the terminally bonded methyl group. The pyridine nitrogen atom and the central ligand nitrogen are placed on the axis [C(19)–V–N(1) = 116.65(6)°, C(19)–V–N(3) = 113.85(7)°, C(19)–V–N(4) = 92.62(5)°, C(19)–V–N(2) = 100.94(5)°]. The coordination geometry around the amido nitrogens is trigonal planar as usual [C(4)–N(1)–Si(1) = 112.9(2)°, C(4)–N(1)–V = 114.2–(2)°, Si(1)–N(1)–V = 128.17(13)°, Si(2)–N(2)–V = 118.73(12)°, C(10)–N(3)–Si(3) = 112.6(2)°, C(10)–N(3)–V = 112.5(2)°], suggesting a substantial extent of V–N  $\pi$ -donation. In agreement, the V–N distances are comparatively short [V–N(1) = 1.972(2) Å, V–N(3) = 1.954(2) Å].

**Complex 3.** The complex is a tetrametallic cluster with two vanadium and two aluminum atoms arranged in two identical subunits each containing one vanadium and one aluminum (Figure 3). The vanadium and aluminum atoms within each subunit are linked together by the silylamino(disilylamido) ligand, while the link between the two subunits is realized by two bridging chlorine atoms [V(1)–Cl(1) = 2.510(2) Å, V(1)–Cl = 2.4815(17) Å, V(1)–Cl(1)–V(2) = 99.36(6)°, Cl–V(1)–Cl(1) = 80.64(6)°]. Each vanadium atom displays a slightly distorted square pyramidal coordination geometry [Cl–V(1)–N(1) = 98.89(12)°, Cl–V(1)–N(3) = 167.9(2)°, Cl–V(1)–Cl(1) = 80.64–(6)°, Cl(1)–V(1)–N(3) = 95.33(16)°]. Two bridging chlorine atoms and two amido nitrogen atoms define the basal plane, while the amino nitrogen atom from the ligand is located on the apical position [N(2)–V(1)–Cl = 110.50(14)°, N(2)–V(1)–N(3) = 81.6(2)°, N(2)–V(1)–N(1) = 81.1(2)°]. Surprisingly, all three V–N bond lengths are quite similar [V(1)–N(1) = 2.217–(5) Å, V(1)–N(2) = 2.224(7) Å, V(1)–N(3) = 2.233(5) Å] despite the different nature of the three nitrogen atoms within each ligand. Two additional dimethylaluminum units are each bound to one silylamino(disilylamido)V moiety via the bridging amido nitrogen atoms [Al–N(1) = 1.958(5) Å, Al–N(3) = 1.954–(6) Å]. The tetrahedral coordination geometry of each aluminum center is thus defined by two terminally bonded methyl groups and two amido nitrogen atoms of the tridentate ligand [N(1)–Al–N(3) = 97.3(2)°, N(1)–Al–C(14) = 112.4(3)°, N(1)–Al–C(15) = 111.3(4)°].

**Complex 4.** The complex is a dinuclear vanadium/aluminum complex with the two metal centers linked by a single bridging chlorine atom [V–Cl(1)–Al = 118.0(6)°] (Figure 4). The coordination geometry around the vanadium atom is slightly distorted trigonal bipyramidal. The equatorial plane is comprised of two terminal nitrogens from the silylamino–(disilylamido) ligand and one terminal chlorine atom [N(1)–

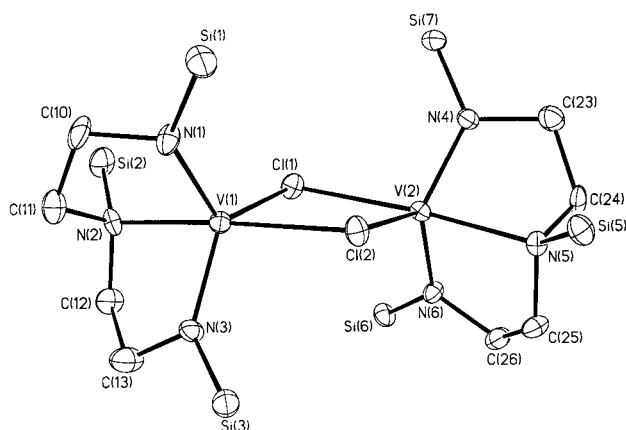
**Table 3. Selected Bond Distances and Angles for Complexes 1, 2, and 3**

1	2	3
V(1)–N(1) = 1.903(6) Å	V–C(19) = 2.118(3) Å	V(1)–Cl(1) = 2.510(2) Å
V(1)–N(2) = 2.179(5) Å	V–N(1) = 1.972(2) Å	V(1)–Cl = 2.4815(17) Å
V(1)–N(3) = 1.902(5) Å	V–N(2) = 2.264(2) Å	V(1)–N(1) = 2.217(5) Å
V(2)–N(4) = 1.906(5) Å	V–N(3) = 1.954(2) Å	V(1)–N(2) = 2.224(7) Å
V(2)–N(5) = 2.188(5) Å	V–N(4) = 2.157(2) Å	V(1)–N(3) = 2.233(5) Å
V(2)–N(6) = 1.909(5) Å		Al–N(1) = 1.958(5) Å
V(1)–Cl(1) = 2.371(2) Å		Al–N(3) = 1.954(6) Å
V(1)–Cl(2) = 2.4592(19) Å		Al–C(14) = 1.970(10) Å
V(2)–Cl(1) = 2.459(2) Å		Al–C(15) = 1.991(9) Å
V(2)–Cl(2) = 2.373(2) Å		
N(1)–V(1)–N(3) = 117.91(26)°	C(19)–V–N(1) = 116.65(6)°	N(2)–V(1)–Cl = 110.50(14)°
N(1)–V(1)–N(2) = 84.69(22)°	C(19)–V–N(3) = 113.85(7)°	N(2)–V(1)–N(3) = 81.6(2)°
N(1)–V(1)–Cl(1) = 119.98(19)°	C(19)–V–N(4) = 92.62(5)°	N(2)–V(1)–N(1) = 81.1(2)°
N(1)–V(1)–Cl(2) = 100.98(17)°	C(19)–V–N(2) = 100.94(5)°	Cl(1)–V(1)–N(1) = 167.9(2)°
N(4)–V(2)–N(6) = 118.03(24)°	C(4)–N(1)–Si(1) = 112.9(2)°	Cl(1)–V(1)–N(3) = 95.33(16)°
N(4)–V(2)–N(5) = 84.76(21)°	C(4)–N(1)–V = 114.2(2)°	N(1)–V(1)–Cl = 98.89(12)°
N(4)–V(2)–Cl(1) = 100.72(17)°	Si(1)–N(1)–V = 128.17(13)°	Cl–V(1)–N(3) = 167.9(2)°
N(4)–V(2)–Cl(2) = 121.96(18)°	Si(2)–N(2)–V = 118.73(12)°	Cl–V(1)–Cl(1) = 80.64(6)°
V(1)–Cl(1)–V(2) = 97.36(6)°	C(10)–N(3)–Si(3) = 112.6(2)°	V(1)–Cl(1)–V(2) = 99.36(6)°
V(1)–Cl(2)–V(2) = 97.44(6)°	C(10)–N(3)–V = 112.5(2)°	N(1)–Al–N(3) = 97.3(2)°
Cl(2)–V(1)–Cl(1) = 82.03(6)°		N(1)–Al–C(14) = 112.4(3)°
Cl(2)–V(2)–Cl(1) = 82.11(6)°		N(1)–Al–C(15) = 111.3(4)°

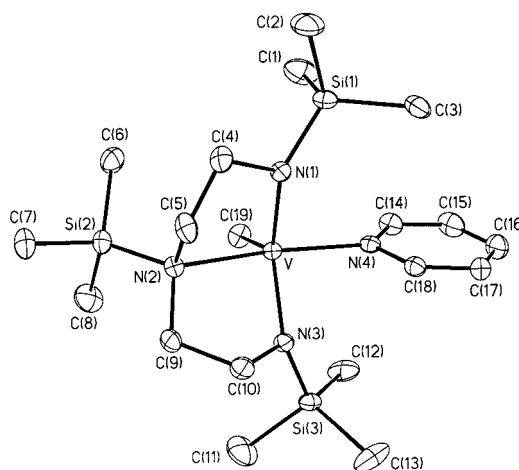
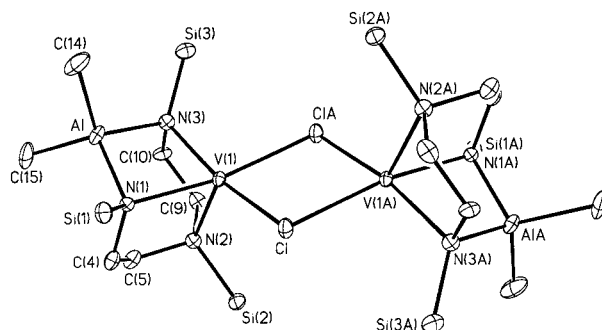
**Table 4. Selected Bond Distances and Angles for Complexes 4 and 5**

4	5
V–N(1) = 1.815(3) Å	V(1)–Cl(1) = 2.412(2) Å
V–N(2) = 2.294(3) Å	V(1)–Cl(2) = 2.389(2) Å
V–N(3) = 1.832(3) Å	V(1)–Cl(3) = 2.389(2) Å
V–Cl(1) = 2.4649(14) Å	V(2)–Cl(1) = 2.453(2) Å
V–Cl(2) = 2.2441(13) Å	V(2)–Cl(2) = 2.456(2) Å
Al–Cl(3) = 2.120(2) Å	V(2)–Cl(3) = 2.460(2) Å
Al–Cl(4) = 2.1070 Å	V(1)–N(1) = 2.150(5) Å
Al–Cl(5) = 2.108(2) Å	V(1)–N(2) = 2.158(5) Å
	V(1)–N(3) = 2.216(5) Å
	Al–N(1) = 1.911(6) Å
	Al–N(3) = 1.914(5) Å
N(1)–V–N(3) = 124.86(14)°	Cl(1)–V(1)–N(1) = 95.37(15)°
N(1)–V–N(2) = 79.80(12)°	Cl(1)–V(1)–N(2) = 178.53(15)°
N(2)–V–Cl(2) = 117.60(11)°	Cl(1)–V(1)–N(3) = 97.83(15)°
N(2)–V–Cl(1) = 95.71(10)°	Cl(1)–V(1)–Cl(3) = 86.03(8)°
V–Cl(1)–Al = 118.0(6)°	Cl(1)–V(2)–Cl(2) = 82.74(7)°
Cl(1)–Al–Cl(3) = 107.13(7)°	Cl(1)–V(2)–Cl(3) = 83.62(8)°
Cl(1)–Al–Cl(4) = 103.46(7)°	Cl(1)–V(2)–Cl(1)#1 = 180.00(1)°
Cl(1)–Al–Cl(5) = 106.32(8)°	Cl(4)–Al–N(1) = 113.12(19)°
	Cl(4)–Al–N(3) = 113.57(18)°
	Cl(4)–Al–Cl(5) = 195.97(11)°

V–N(3) = 124.86(14)°, N(1)–V–N(2) = 79.80(12)°, N(2)–V–Cl(2) = 117.60(11)°, N(2)–V–Cl(1) = 95.71(10)°]. The chlorine atom that bridges vanadium to aluminum, and the central

**Figure 1.** ORTEP plot of **1**. Thermal ellipsoids are drawn at 30% probability level. Carbon atoms of the trimethylsilyl groups have been omitted for clarity.

silylamine nitrogen atom occupy the axial positions [N(2)–V–Cl(1) = 170.63(8)°]. The nearly regular tetrahedral environment around Al is defined by three terminal and one bridging chlorine atom [Cl(1)–Al–Cl(3) = 107.13(7)°, Cl(1)–Al–Cl(4) = 103.46(7)°, Cl(1)–Al–Cl(5) = 106.32(8)°]. The V–N distances [V–N(1) = 1.815(3) Å, V–N(3) = 1.832(3) Å] are normal and compare well with those of complex **1**. The vanadium silylamine distance is instead substantially longer [V–N(2) = 2.294(3) Å]. The V–Cl distances [V–Cl(1) = 2.4649(14) Å, V–Cl(2) = 2.2441(13) Å] differ slightly from each other, with

**Figure 2.** ORTEP plot of **2**. Thermal ellipsoids are drawn at 30% probability level.**Figure 3.** ORTEP plot of **3**. Thermal ellipsoids are drawn at 30% probability level. Carbon atoms of the trimethylsilyl groups have been omitted for clarity.



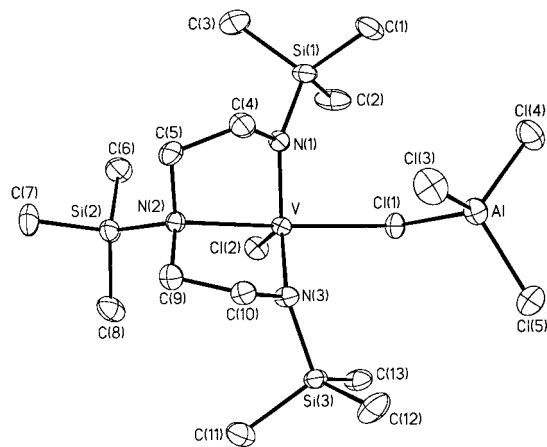


**Figure 4.** ORTEP plot of **4**. Thermal ellipsoids are drawn at 30% probability level.

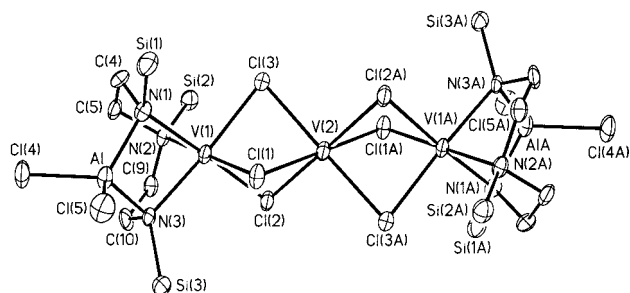


**Figure 5.** ORTEP plot of **5**. Thermal ellipsoids are drawn at 30% probability level. Carbon atoms of the trimethylsilyl groups have been omitted for clarity.

the bridging chlorine forming a longer distance. A similar trend is observed for the Al–Cl distances with terminal chlorine atoms having slightly shorter Al–Cl distances [Al–Cl(3) = 2.120(2) Å, Al–Cl(4) = 2.1070 Å, Al–Cl(5) = 2.108(2) Å] than the bridging Al–Cl distance [Cl(1)–Al = 2.1971(18) Å].

**Complex 5.** The structure is a symmetry-generated pentametallic cluster composed by three vanadium atoms and two aluminum residues located at the periphery of the molecule (Figure 5). The three hexacoordinated vanadium atoms are arranged to form a linear trimetallic unit. The central vanadium, located on the inversion center, is surrounded by six chlorides [V(2)–Cl(1) = 2.453(2) Å, V(2)–Cl(2) = 2.456(2) Å, V(2)–Cl(3) = 2.460(2) Å], which fill the six coordination sites and provide the metal with a rather regular antiprismatic geometry [Cl(1)–V(2)–Cl(2) = 82.74(7)°, Cl(1)–V(2)–Cl(3) = 83.62(8)°, Cl(1)–V(2)–Cl(3)#1 = 180.00(1)°]. The other two vanadium atoms are located at either side of the central vanadium and share three chlorine atoms each [V(1)–Cl(2) = 2.389(2) Å, V(1)–Cl(3) = 2.389(2) Å] in a slightly distorted octahedral coordination geometry [Cl(1)–V(1)–N(1) = 95.37(15)°, Cl(1)–V(1)–N(2) = 178.53(15)°, Cl(1)–V(1)–N(3) = 97.83(15)°, Cl(1)–V(1)–Cl(3) = 86.03(8)°]. The equatorial plane is defined by two of the three bridging chlorine atoms and the two terminal amido nitrogen atoms [V(1)–N(1) = 2.150(5) Å, V(1)–N(3) = 2.216(5) Å]. The third chlorine atom [V(1)–Cl(1) = 2.412(2) Å] and the central nitrogen atom [V(1)–N(2) = 2.158(5) Å] of the ligand occupy the two axial positions. The fact that one chlorine atom is in the axial versus the equatorial position with respect to the peripheral vanadium atom determines the antiprismatic distortion of the octahedral geometry of the central vanadium atom. Two AlCl<sub>2</sub> units are located at the exterior of the trivanadium unit each connected to one of the two external vanadium atoms. Each aluminum atom is bonded to the two amido ligand nitrogen atom bonds [Al–N(1) = 1.911(6) Å, Al–N(3) = 1.914(5) Å], while two terminally bonded chlorine atoms complete the distorted tetrahedral

geometry [Cl(4)–Al–N(1) = 113.12(19)°, Cl(4)–Al–N(3) = 113.57(18)°, Cl(4)–Al–Cl(5) = 195.97(11)°].

## Results and Discussion

The preparation of [ $\{V(\text{Me}_3\text{Si})\text{N}\{\text{CH}_2\text{CH}_2\text{N}(\text{SiMe}_3)\}_2\}_2\text{-}(\mu\text{-Cl})_2$ ] (**1**) as a red-violet crystalline material was carried out according to the procedure recently described by Cloke<sup>6,8</sup> via room-temperature reaction of  $\text{Li}_2[(\text{Me}_3\text{Si})\text{N}\{\text{CH}_2\text{CH}_2\text{N}(\text{SiMe}_3)\}_2]$  with  $\text{VCl}_3(\text{THF})_3$  in THF. The structure unequivocally confirmed the dinuclear nature of **1** with the two trigonal bipyramidal vanadium centers linked by two bridging chlorine atoms (Figure 1).

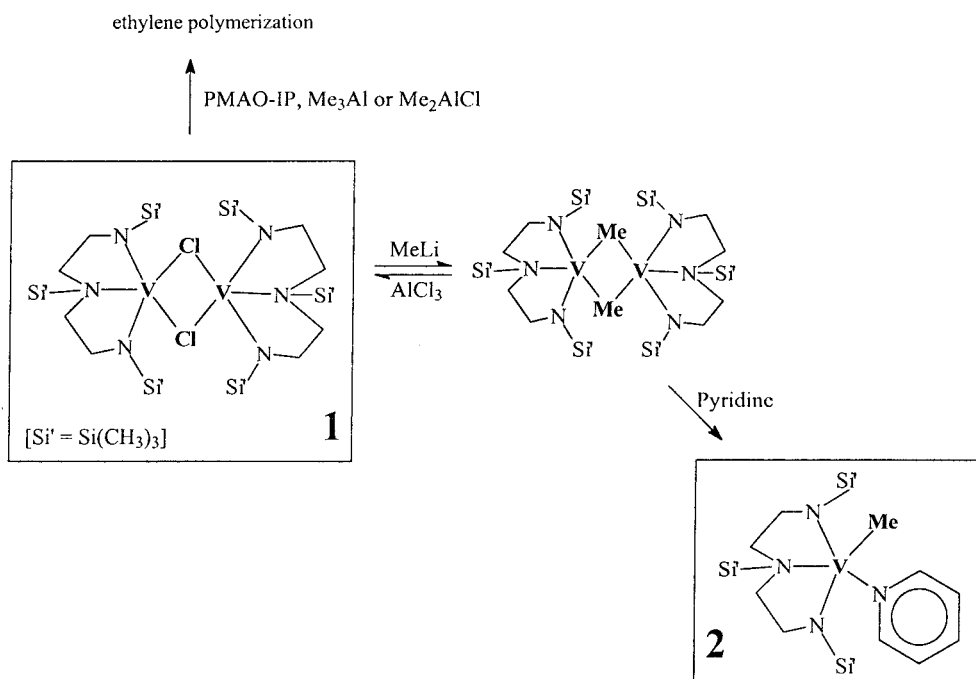
While activated by 60 equiv of  $\text{Me}_2\text{AlCl}$ ,  $\text{Me}_3\text{Al}$ , or PMAO-IP, complex **1** displayed a substantial activity as an ethylene polymerization catalyst. The activity obtained with PMAO-IP activation (237 g of PE/mmol/h) was 20 times higher than in the case of  $\text{Me}_3\text{Al}$ , while the highest activity was obtained with  $\text{Me}_2\text{AlCl}$ . The polymers obtained from the different activators and under comparable reaction conditions were very similar. The catalytic activity recorded for polymerization experiments carried out with  $\text{Me}_2\text{AlCl}$  at 50 °C and under 300 psig of ethylene was 660 g of PE/mmol/h. The polyethylene showed catalyst unimodality with average molecular weight of 721 000 and polydispersity of 2.3 (see Supporting Information Figure S1). The melting point of the polymer (133.95 °C) indicated that the polyethylene was essentially linear. Not surprising for a vanadium catalyst, the activity decreased at higher temperature (237 g of PE/mmol/h at 140 °C, 286 psig). Also the polymer displayed lower average molecular weight (135 700) but similar polydispersity (2.7) and the presence of a significant fraction of higher molecular weight polymer (see Supporting Information Figure S2), indicating that catalyst bimodality takes place at higher temperatures.

In common with other vanadium catalysts, **1** is short-lived at either 35 or 140 °C, typically not remaining active for more than 20–30 min, the longest catalyst life having been observed at 50 °C. Such deactivation is usually attributed to reduction of the vanadium center to the inactive divalent state. The reduction is thought to involve loss of the polymeric alkyl chain and is believed to be due to an intrinsic instability of the vanadium–carbon bond. However, we have reported that amide ligands may stabilize tetravalent vanadium alkyls,<sup>16</sup> while, by using the silylamino(disilylamido) ligand, Cloke has isolated a mononuclear trimethylsilylmethyl derivative and successfully hydrogenolyzed it to produce the corresponding dinuclear and trivalent vanadium hydride.<sup>8</sup> In all these reactions there was no indication of reduction of the vanadium center, suggesting that amide ligands indeed provide sufficient stabilization to the V–C function.

Nevertheless, the rapid catalyst failure and the fact that the alkyl derivatives of this system reported before are particularly bulky prompted us to further investigate the ability of this versatile ligand system to support more standard vanadium-alkyls. Complex **1** undergoes a rapid reaction with MeLi in hexane resulting in the formation of a grayish precipitate (LiCl) and yielding a

(16) Desmangles, N.; Gambarotta, S.; Bensimon, C.; Davis, S.; Zahalka, H. *J. Organomet. Chem.* **1997**, *562*, 53.

## Scheme 1



complex that was tentatively assigned as a methyl-bridged dimer  $[\{V(\text{Me}_3\text{Si})\text{N}\{\text{CH}_2\text{CH}_2\text{N}(\text{SiMe}_3)\}_2\}(\mu\text{-Me})_2]$  probably of very similar structure to **1**. Unfortunately, despite repeated attempts we were unable to obtain crystals suitable for an X-ray diffraction study. However, given the release of nearly a stoichiometric amount of methane gas during degradation experiments carried out with gaseous HCl in a closed vessel connected to a Toepler pump, a structure with methyl bridges seems the most likely. Furthermore, treatment of the reaction solution with AlCl<sub>3</sub> re-formed the starting material **1** in good yield (Scheme 1), and simple addition of pyridine gave red crystals of  $[(\text{Me}_3\text{Si})\text{N}\{\text{CH}_2\text{CH}_2\text{N}(\text{SiMe}_3)\}_2\text{V}(\text{Me})(\text{Py})]$  (**2**) in good yield. The X-ray crystal structure revealed that **2** is mononuclear and that it has a terminally bonded Me group (Figure 2). Complex **2** and its precursor enlarge the meager list of examples of stable V(III)-alkyl complexes.<sup>5,8</sup> Both are thermally robust since no decomposition was observed in boiling toluene, and their unusual stability is likely to be ascribed to the particular nature of the amide ligand.

The versatility of the silylamino silyldiamide ligand to stabilize the vanadium carbon bond reiterates questions about the factors determining the catalyst failure. One possibility, although unlikely, is that the ligand might be leached out of the metal center by the aluminum cocatalyst with a consequent decrease of the stability of the V–C bond. To rule out this possibility, we studied the interaction of **1** with the aluminum cocatalyst in the hope of trapping some vanadium–aluminum species. The reaction of **1** with either PMAO-IP, AlMe<sub>3</sub>, or Me<sub>2</sub>AlCl in hexane initially gave a red solution, which after a few days afforded emerald-green crystals of the tetrametallic ( $[\{(\text{Me}_3\text{Si})(\text{AlMe}_2)\text{NCH}_2\text{CH}_2\}_2\text{N}(\text{SiMe}_3)\}_2\text{V}_2(\mu\text{-Cl})_2$ ) (**3**) (Scheme 2). As expected, the best yield was obtained with Me<sub>3</sub>Al. The X-ray crystal structure clearly showed that the ligand remains triply bound to the vanadium center. The main frame of the complex is virtually the same as in **1**, with the two ( $[\{(\text{Me}_3\text{Si})\text{NCH}_2\text{CH}_2\}_2\text{N}(\text{SiMe}_3)\}_2\text{V}$ ) moieties held

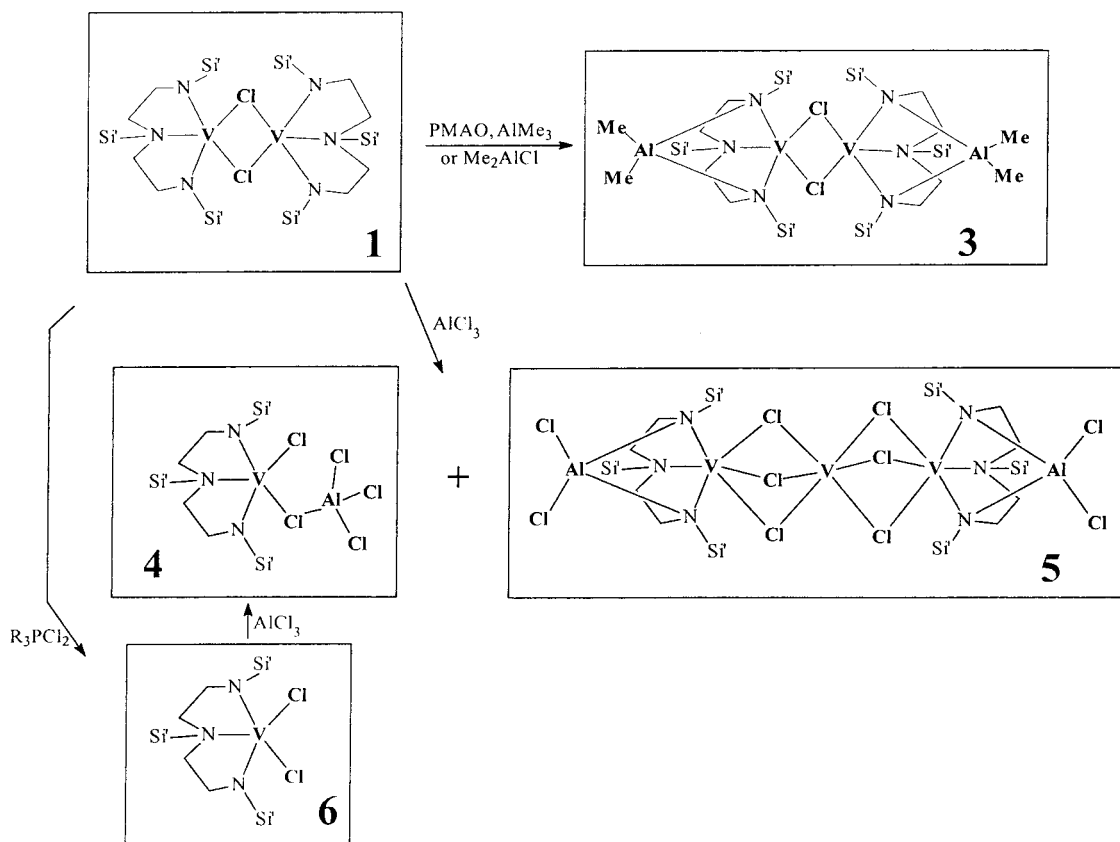
together by two bridging chlorines. However, there are two major differences. First, two Me<sub>2</sub>Al residues are now coordinated each to one ligand's amide nitrogen atom. Second, the vanadium center has been reduced to the inactive divalent state, thus accounting for the catalyst failure. The magnetic moment of 3.9 μ<sub>B</sub>/vanadium is as expected for the high-spin d<sup>3</sup> electronic configuration of a divalent vanadium center.

The isolation and characterization of **3** indicates that no ligand leaching occurs in the present catalytic system but rather aggregation with the cocatalyst. Yet, the vanadium center was reduced to the inactive divalent state. Thus, questions arise about how the reduction occurred given that simple chlorine replacement by Me groups afforded thermally stable trivalent methyl derivatives.

In Ziegler–Natta catalysis, PMAO or AlR<sub>3</sub> in general plays a dual role as both an alkylating agent and a Lewis acid. To separately analyze these two different aspects of the aluminum derivatives, we reacted **1** with AlCl<sub>3</sub>, a pure Lewis acid, with no possibility of functioning as a reducing agent. The reaction was carried out in toluene (Scheme 2) and afforded a brown solution, from which a mixture of two different compounds was obtained. X-ray diffraction of the crystals of the major component revealed the structure to be the hetero-bimetallic and tetravalent  $[(\text{Me}_3\text{Si})\text{N}\{\text{CH}_2\text{CH}_2\text{N}(\text{SiMe}_3)\}_2\text{V}(\text{Cl})(\mu\text{-Cl})\text{AlCl}_3]$  (**4**), which is basically the result of the coordination of AlCl<sub>3</sub> to the tetravalent  $[(\text{Me}_3\text{Si})\text{N}\{\text{CH}_2\text{CH}_2\text{N}(\text{SiMe}_3)\}_2\text{VCl}_2]$  via sharing of one of the two vanadium chlorine atoms (Figure 4). The tetravalent oxidation state of vanadium was also confirmed by the measurement of the magnetic moment, which is consistent with a d<sup>1</sup> electronic configuration (1.83 μ<sub>B</sub>).

The second component of the reaction mixture is particularly intriguing. The complex is a mixed-valence V(II)/V(III) hetero-bimetallic pentamer  $[\{[(\text{SiMe}_3)(\text{AlCl}_2)\text{NCH}_2\text{CH}_2\}_2(\text{Me}_3\text{Si})\text{NV}\}(\mu\text{-Cl})_3\text{V}(\mu\text{-Cl})_3\{(\text{SiMe}_3)(\text{AlCl}_2)\text{NCH}_2\text{CH}_2\}_2(\text{Me}_3\text{Si})\text{NV}\}] \cdot (\text{toluene})_2$  (**5**), in which there

Scheme 2



are two vanadium atoms *formally* in the +3 oxidation state and one in the +2 (Figure 5). Unfortunately, while complex **4** was obtained in analytically pure form, samples of **5** were invariably contaminated by variable amounts of **4**, thus preventing a satisfactory analytical characterization.

The simultaneous formation of both **4** and **5** clearly indicates that AlCl<sub>3</sub> triggers a disproportionation reaction through which V(II) and V(IV) species are formed. The fact that the central vanadium atom in complex **5** has been stripped of the ligand system clearly indicates that ligand leaching still occurred despite the ligand tridenticity and the higher affinity of vanadium for nitrogen donor atoms compared to aluminum. However, the fact that two AlCl<sub>2</sub> residues are connected to the periphery of the trimetallic cluster in a fashion that is identical to the coordination of the AlMe<sub>2</sub> residues in **3** indicates that (1) the ligand leaching is only partial and probably governed by an equilibrium; (2) there is a common trend in the behavior of **1** with both Me<sub>3</sub>Al and AlCl<sub>3</sub>.

Complex **5** may be regarded as resulting from the *formal* aggregation of **1** with AlCl<sub>3</sub> and VCl<sub>2</sub> residues obviously generated as a partner of the oxidation to **4**. Thus, it is tempting to rationalize the formation of the mixture of **4** and **5** in terms of initial partial reaction of **1** with AlCl<sub>3</sub> to afford VCl<sub>3</sub> and [(Me<sub>3</sub>Si)N{CH<sub>2</sub>CH<sub>2</sub>N(SiMe<sub>3</sub>)<sub>2</sub>Al(Cl)}] (Scheme 3). The association of VCl<sub>3</sub> with **1** triggers a disproportionation to the tetravalent [(Me<sub>3</sub>Si)N{CH<sub>2</sub>CH<sub>2</sub>N(SiMe<sub>3</sub>)<sub>2</sub>VCl<sub>2</sub>}] (**6**) and "VCl<sub>2</sub>". This residue may react with both unreacted **1** and AlCl<sub>3</sub> to form **5**. In agreement with this proposal, reaction of **1** with anhydrous VCl<sub>3</sub> in toluene indeed afforded a mixture of **6** (isolated from crystallization from hexane)

and a poorly soluble residue, which was redissolved in boiling THF and precipitated upon treatment with TMEDA and identified as VCl<sub>2</sub>(TMEDA)<sub>2</sub>.<sup>17</sup> Finally, complex **6**, which was conveniently obtained via oxidation of **1** with Ph<sub>3</sub>PCl<sub>2</sub>, reacted with AlCl<sub>3</sub> to afford **4**.

Thus, the isolation of both tetra- and divalent vanadium species in the reaction of **1** with AlCl<sub>3</sub> clearly indicates that a disproportionation is at the basis of the reduction of the vanadium center. However, the fact that a vanadium atom in **3** has retained its ligand system and yet has been reduced strongly suggests that no ligand leaching occurred during the reaction of **1** with AlMe<sub>3</sub>, as it can be expected given its lower Lewis acidity. Thus, the only possibility to explain the reduction of the metal center in the case of **3** is to assume that the addition intermediate (Me<sub>2</sub>Al){(Me<sub>3</sub>Si)N[CH<sub>2</sub>CH<sub>2</sub>N(SiMe<sub>3</sub>)<sub>2</sub>]VClMe}, which is also likely to be the catalytically active species, has an intrinsic instability of the V–C bond (Scheme 4). Accordingly, a substantial amount of methane and a small amount of ethane was identified in the GC of the reaction mother liquor.

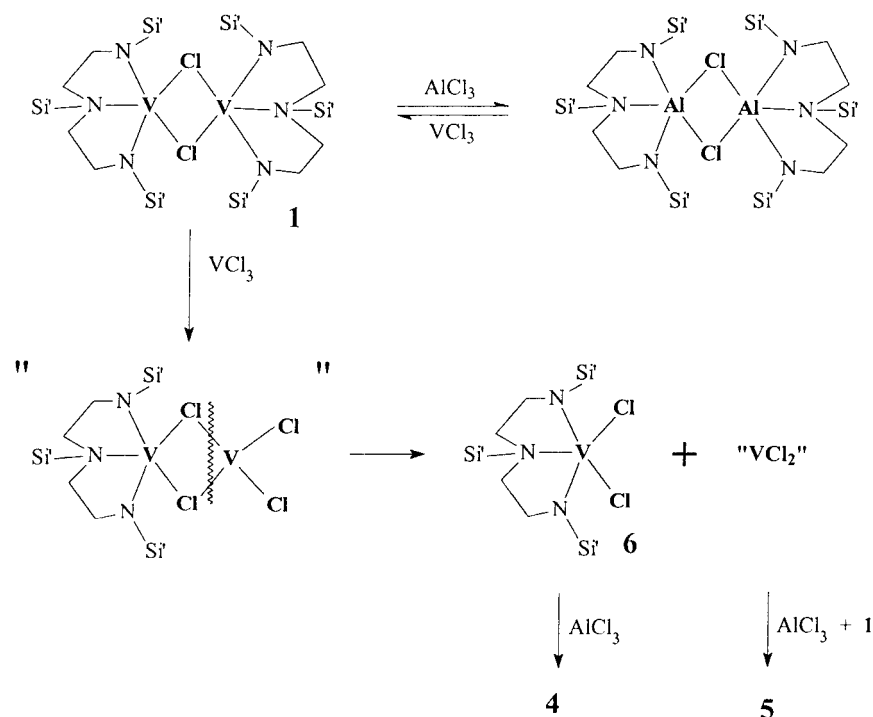
## Conclusions

This work has allowed the isolation of a few novel vanadium aluminum clusters supported by the trimethylsilylamino(trimethylsilyldiamido) ligand. While the ligand system is capable of aggregating vanadium and aluminum residues, the complete abstraction of ligand from vanadium, responsible for triggering disproportionation toward di- and tetravalent vanadium, is

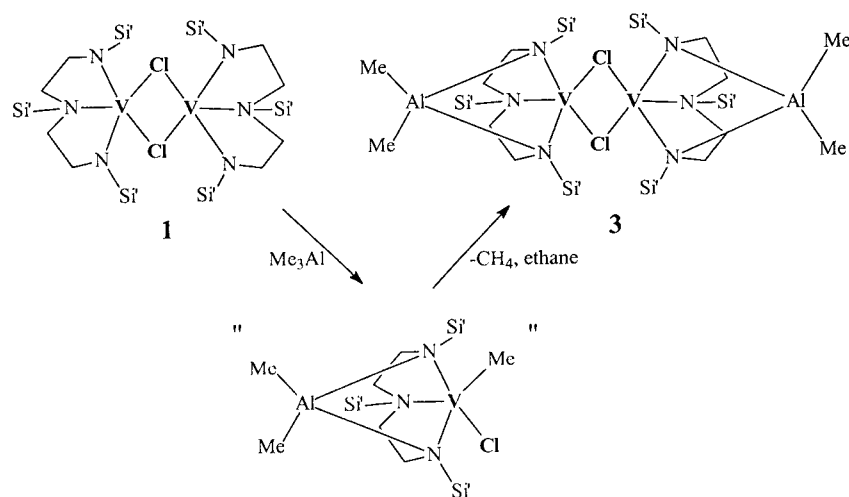
(17) Edema, J. J. H.; Stauffer, W.; Gambarotta, S.; van Bolhuis, F.; Smets, W. W. J.; Spek, A. *Inorg. Chem.* **1990**, *29*, 1302.



Scheme 3



Scheme 4



determined by the Lewis acidity of the aluminum cocatalyst, i.e., the chlorine content. Despite the ability of this ligand system to stabilize both mono- and dinuclear trivalent vanadium alkyl derivatives and even in the event where ligand leaching did not occur, the vanadium atom can still be reduced. This is likely due to an intrinsic instability of the V–C bond of an alkyl/halide intermediate. Thus, the design of long-lasting vanadium catalysts remains determined by the understanding of the factors affecting the stability of the V–C bond.

**Acknowledgment.** This work was supported by the National Science and Engineering Research Council of Canada (NSERC) and by NOVA Chemicals (Calgary, Canada). We are also indebted to Prof. S. Collins (Waterloo) for making available his HT-GPC facility.

**Supporting Information Available:** Crystallographic tables for all the compounds reported in this work, additional figures, and figure for the differential molecular weight distribution. This material is available free of charge via the Internet at <http://pubs.acs.org>.

OM011040U